Gamma-Ray Irradiation and Post-Irradiation Responses of High Dose Range RADFETs

A. Jaksic, G. Ristic, M. Pejovic, A. Mohammadzadeh, C. Sudre, and W. Lane

Abstract-- **Gamma-ray irradiation and post-irradiation responses have been studied for the two types of radiation sensitive p-channel MOSFETs (RADFETs) from different manufacturers. In addition to, in dosimetric applications standard, threshold voltage measurements at a single specified current, transistor I-V and charge-pumping characteristics have been monitored. This has been shown to be useful in providing a more detailed insight into processes that occur during irradiation and subsequent annealing at elevated temperature. In particular, the role of switching oxide traps (also known as "border" traps) and electron traps in studied devices has been revealed.**

I. Introduction

SINCE the introduction of the space charge dosimeter concept [1], radiation sensitive p-channel MOSFETs (also known as RADFETs) have been developed for applications such as space, nuclear industry and research, and radiotherapy [1-4]. Other types of dosimeters that are commonly used or are being developed for these applications include thermoluminescent dosimeters (TLDs), semiconductor diodes, and optically stimulated luminescence dosimeters (OSDLs). A comprehensive review of radiation dosimetry issues and devices can be found in [5]. The TLDs are rather small, well characterised and standard in use, however, they are not suitable for remote measurements and the read-out of dosimetric information is destructive. Semiconductor diodes are also miniature in size, but produce small dosimetric signal and require high voltage. The OSL dosimetry concept has re-emerged recently with promising results [6,7], however OSLDs require integration of electronics and optic elements in the read-out system and dosimetric information is read destructively. The RADFET advantages include immediate, non-destructive read-out of dosimetric information, extremely small size, very low power consumption, all-electronic interfaces fully compatible with microprocessors, high dose range and very competitive price. The RADFET disadvantages are a need for calibration in different radiation fields, relatively low resolution (starting from about 1 rad) and non-reusability. A new design approach has been investigated recently that could overcome the low resolution problem and introduce the RADFETs into the personnel dosimetry area [8].

The NMRC have been active in RADFET research and development since late 1980's, resulting in a range of commercially available RADFETs for various applications [9], i.e. different dose ranges. This paper will present and discuss the irradiation and post-irradiation response of low sensitivity/high dose range RADFETs. These RADFETs typically have about 100nm thick gate oxides (gate oxide of high sensitivity/low dose range RADFETs can be up to 1 μm thick) and are suitable for space and nuclear research/industry applications. We will examine the RADFET response in the space dose range, i.e. up to the total absorbed doses of several hundred Gy (1 Gy = 100 rad). The responses of devices from two different manufacturers will be compared.

Radiation induces charge trapping in the gate oxide and at the Si/SiO_2 interface, causing the threshold voltage shift (ΔV_T), which is the RADFET dosimetric parameter. There are several definitions of the MOSFET threshold voltage (V_T) [10], however, the one that is most commonly used in RADFET applications is that the V_T is the voltage needed to sustain a specified current. Thus, the V_T is measured at a single point of the transfer I-V characteristics, applying a specified current (typically in the order of ten μA) to the RADFET in two-terminal mode (source and bulk are shorted and represent one terminal, while drain and gate are also shorted and represent another terminal). This configuration will be referred to as a Reader Circuit (RC) configuration and is shown in Fig. 1. While, for its simplicity, the RC configuration is suitable for practical applications and calibration measurements, it doesn't provide the quantification of and insight into the charge trapping mechanisms that could serve as the basis for RADFET fabrication process improvements. For this reason we have performed I-V and charge-pumping (CP) measurements in addition to the RC measurements. This has enabled us to analyse basic mechanisms underlying irradiation and post-irradiation behaviours of the RADFETs and, in particular, discuss the role of switching oxide traps in studied devices.

A. Jaksic is with the National Microelectronics Research Centre, Cork, Ireland (e-mail: ajaksic@nmrc.ie).

G. Ristic is with the Sunnybrook Health Science Center, University of Toronto, Canada (e-mail: gristic@sten.sunnybrook.utoronto.ca).

M. Pejovic is with the Faculty of Electronic Engineering, University of Nis, Yugoslavia (e-mail: pejovic@elfak.ni.ac.yu).

A. Mohammadzadeh is with European Space Agency (ESA/ESTEC), Noordwijk, the Netherlands (e-mail: ali.mohammadzadeh@esa.int).

C. Sudre was with the National Microelectronics Research Centre, Cork, Ireland. He is now with General Semiconductors, Freiburg, Germany (e-mail: csudre@gensemi.com)

W. Lane was with the National Microelectronics Research Centre, Cork, Ireland. He is now with Analog Devices, Cork, Ireland (e-mail: bill.lane@analog.com).

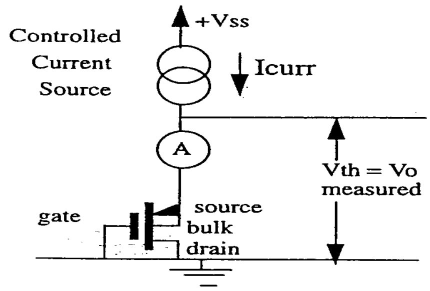

Fig. 1. Reader Circuit (RC) configuration for threshold voltage measurements in RADFETs; Icurr=10μA was used.

II. Experimental Details

The RADFETs from two different manufacturers (NMRC, Ireland, and EI-Microelectronics, Yugoslavia) have been investigated. Both types of devices are p-channel MOSFETs fabricated in Al-gate process. The NMRC RADFETs have 100nm thick gate oxide, grown at 1000°C in dry oxygen, and annealed for 15 minutes at 1000°C in nitrogen. The post-metallisation anneal (PMA) was performed at 440°C in forming gas for 60 minutes. The EI RADFETs [11] have 110nm thick gate oxide, grown at 1150°C in wet oxygen, and annealed for 60 minutes at 1050°C in nitrogen. The 30 minute PMA was done at 440°C in forming gas.

Experimental samples were irradiated at room temperature using the Co-60 source to 300 Gy at the dose rate of 0.013 Gy/s. All doses are given in Gy(H_2O), to convert to Gy(SiO_2) ≈ Gy(Si), one has to multiply the dose by 0.898. The gate bias during irradiation (V_{irr}) was either 0 or +5V. Immediately after irradiation, the devices were annealed at 100°C with –10, 0 or +10V annealing bias (V_{ann}). There were at least two (and in many cases more) samples for each annealing experimental condition in terms of V_{irr}/V_{ann} values. The discrepancies between nominally identical samples were in all cases within 5%. The V_T values were determined using the RC configuration with 10 μA current (Fig. 1). In addition, device transfer I-V characteristics in saturation were recorded, enabling determination of the "extrapolated" V_T and channel mobility (μ) [10]. The densities of radiation-induced fixed traps (ΔN_{ft}[cm^{-2}]) and switching traps (ΔN_{st}[cm^{-2}]) were determined from the sub-threshold I-V curves using the midgap technique (MGT) of McWhorter and Winokur [12]. Finally, the charge-pumping technique (CPT) measurements [13] were performed to determine the energetic densities of switching traps (ΔD_{st}[cm^{-2}eV^{-1}]), $\Delta N_{st}=\Delta D_{st}\times\Delta E$, where ΔE[eV] is an energy range within the Si band-gap scanned by the measurement. Parameters of the CP measurements (recording of Elliot-type CP curves [14], triangular pulse, frequency 100kHz, amplitude 4V, duty cycle 50%) were such that CPT and MGT scanned regions within the silicon band-gap of the same energetic widths (approx. 0.43 eV). Thus, the ΔN_{st} values obtained by MGT and CPT will be directly compared in this paper.

Note that the terms "fixed" and "switching" are used here to define the electrical response of the traps: while fixed traps do not exchange charge with the Si during the time frame of the measurement, switching traps do. Thus, fixed traps cause parallel shift in sub-threshold transfer I-V characteristics (MGT) or Elliot-type CP curves (CPT). Switching traps result in an increase of the sub-threshold slope (MGT) or of the CP current (CPT). As to the location of these traps, fixed traps are located exclusively in the oxide, while switching traps can be exactly at the Si/SiO_2 interface (interface traps, density ΔN_{it}[cm^{-2}]) or in near-interfacial region of the oxide (switching oxide traps, also known as border traps [15], density ΔN_{sot}[cm^{-2}]). Thus, the oxide traps include fixed oxide traps and switching oxide traps, and their total density can be expressed as $\Delta N_{ot}=\Delta N_{ft}+\Delta N_{sot}$. The above described nomenclature was adopted as it better suits the nature of measurements that were done on the experimental samples. Namely, both MG and CP are electrical measurements that can distinguish the radiation-induced defects by their electrical response rather than by location. More details on this will follow in the next Section.

III. Results and Discussion

A. Irradiation

Figs. 2 and 3 show extrapolated and reader circuit ΔV_T during irradiation for NMRC and EI samples, respectively. The agreement between extrapolated and reader circuit ΔV_T is very good (within 1-2%) in all cases, justifying the use of the RC configuration in practical applications. The radiation sensitivities determined at 300 Gy are given in Table 1.

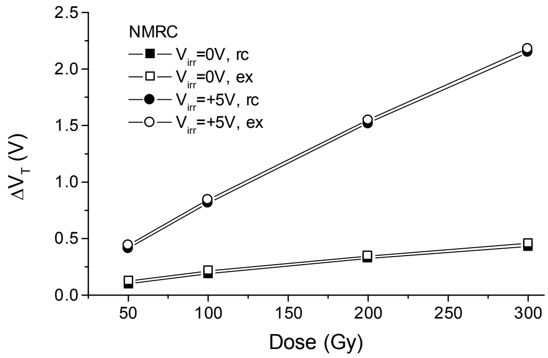

Fig. 2. NMRC samples: reader circuit (rc) and extrapolated (ex) ΔV_T during irradiation with zero and positive gate bias.

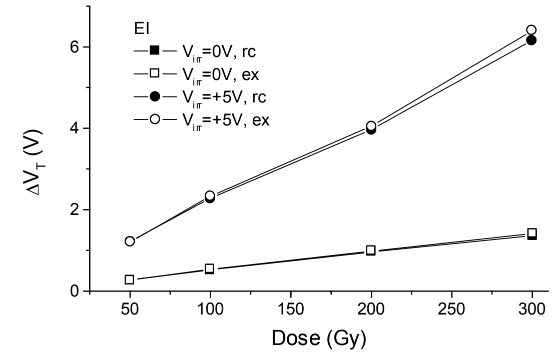

Fig. 3. EI samples: reader circuit (rc) and extrapolated (ex) ΔV_T during irradiation with zero and positive gate bias.

TABLE I
NMRC AND EI SAMPLES: SENSITIVITY FIGURES
([MV/CGY] AT 300 GY(H_2O))

	V_{irr}=0V	V_{irr}=+5V
NMRC	0.015	0.071
EI	0.047	0.217

The EI samples have roughly a factor of 3 higher sensitivity for both V_{irr} conditions. Only a small fraction of the difference can be attributed to somewhat greater oxide thickness of the EI samples (110nm vs. 100nm in the NMRC samples). By far the most of the sensitivity difference comes from charge trapping properties of EI RADFET gate oxide (see below for more details). Note that the high sensitivity may not necessarily be an advantage, particularly in very high dose applications, as it will reduce the maximum detectable dose [2].

Fig. 4 shows the changes in μ, normalised to pre-irradiation value (μ_o), during irradiation. There is almost no change in μ in NMRC samples, while there is a large μ decrease, enhanced by positive V_{irr}, in EI samples.

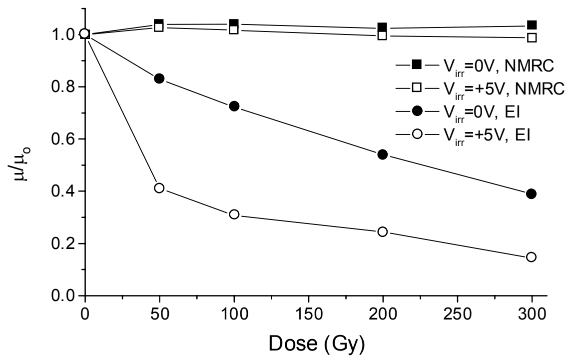

Fig. 4. NMRC and EI samples: μ/μ_o during irradiation with zero and positive gate bias.

Figs. 5 and 6 show ΔN_{ft} and ΔN_{st} during irradiation for NMRC and EI samples, respectively. As expected, positive V_{irr} enhances formation of both fixed and switching traps. The MGT and CPT data are in qualitative agreement, but the ΔN_{st}(CPT) is in all cases lower than ΔN_{st}(MGT). The exact quantitative agreement should not be expected for at least two reasons. First, the two techniques have different effective frequencies: a few Hz (MGT) vs. 100kHz (CPT). Both MGT and CPT are capable of sensing the interface traps, which are very fast, but the contributions of switching oxide traps to the CP and MG signals are not the same. While MGT senses almost all switching oxide traps (slow, medium fast and fast), the CP signal in our case excludes at least contributions of slow and medium fast switching oxide traps, and, consequently, ΔN_{st}(CPT) is expected to be lower. Second, the two techniques scan different portions of the Si band gap: lower half (MGT) vs. central portion (CPT). As interface traps have an U-shaped distribution towards the edges of the band gap [10,16] and that portion can not be reached by CPT, this is an additional reason that may lead to the lower ΔN_{st}(CPT) values. The ΔN_{ft} dominates in NMRC samples (at 300 Gy, $\Delta N_{ft}/\Delta N_{st}$ equals 1.9 for V_{irr}=0V, and 3.7 for V_{irr}=+5V). However, in EI samples, ΔN_{st}(MGT) even exceeds ΔN_{ft}. Thus, the greater sensitivity of EI samples is mostly due to the enhanced formation of switching traps (i.e. switching oxide traps and interface traps). It is probable that some portion (NMRC samples) or even most of the ΔN_{ft} determined by MGT (EI samples) is due to switching oxide traps [17] (see discussion further below).

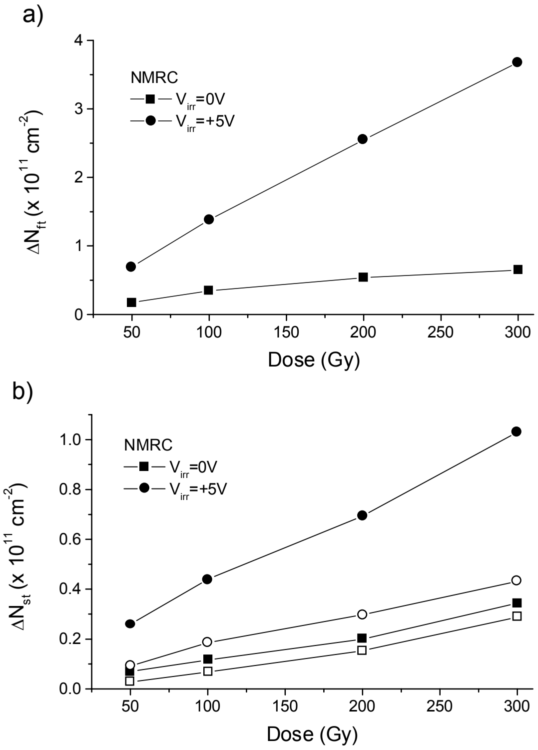

Fig. 5. NMRC samples: ΔN_{ft} (a) and ΔN_{st} (b; MG-solid symbols, CP-open symbols) during irradiation with zero and positive gate bias.

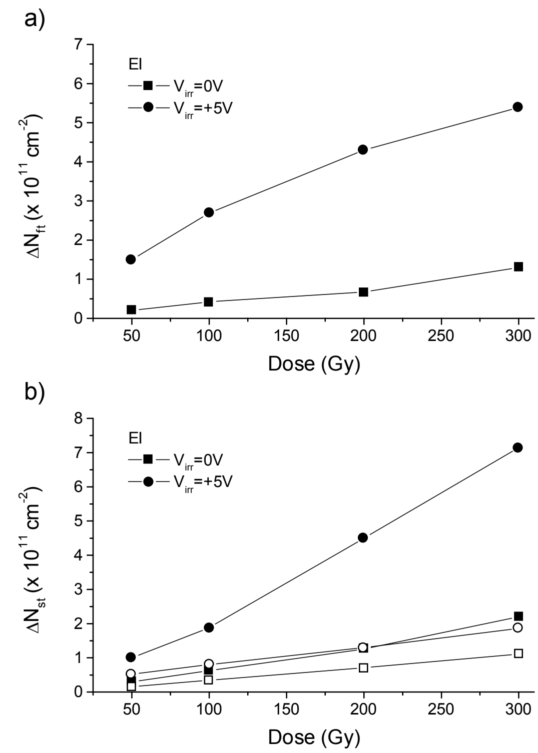

Fig. 6. EI samples: ΔN_{ft} (a) and ΔN_{st} (b; MG-solid symbols, CP-open symbols) during irradiation with zero and positive gate bias.

The CPT provides means for estimating not only ΔN_{st}, but also the absolute switching trap densities (N_{st}). The pre-irradiation N_{st} values are $(1.18 \pm 0.03) \times 10^{10}$ $cm^{-2}eV^{-1}$ in NMRC samples, and $(0.42 \pm 0.09) \times 10^{10}$ $cm^{-2}eV^{-1}$ in EI samples. While pre-irradiation N_{st} is higher in the NMRC samples, the fabrication process is better controlled in this respect than the EI one, with much lower N_{st} variations between the samples. The range of N_{st} increase after irradiation in NMRC samples is 4-5 times, while in EI samples it is 30-50 times.

B. Annealing

Figs. 7 and 8 show ΔV_T evolution during annealing for NMRC and EI samples, respectively. The ΔV_T behaviour depends primarily on V_{ann}. It is interesting to note that in both samples, the loss of dosimetric information (fading) is more pronounced for zero than for positive V_{ann}.

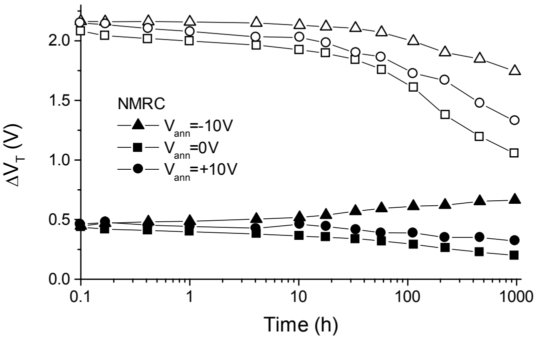

Fig. 7. NMRC samples: ΔV_T during annealing at 100°C with negative, zero and positive gate bias; solid symbols - zero irradiation bias, open symbols - positive irradiation bias (+5V).

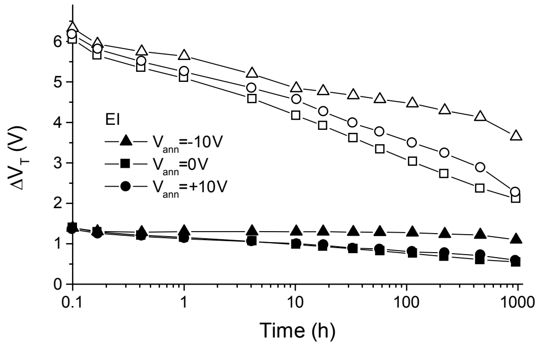

Fig. 8. EI samples: ΔV_T during annealing at 100°C with negative, zero and positive gate bias; solid symbols - zero irradiation bias, open symbols - positive irradiation bias (+5V).

The μ/μ_o evolution during annealing is shown in Figs. 9 and 10. One of the intentions of our study was to determine the effect of fixed oxide traps on μ in p-channel MOSFETs. Namely, it has been unambiguously established that interface traps have predominant effect on μ, acting to decrease μ in both n-channel and p-channel devices [18,19]. The effect of fixed oxide traps in n-channel devices is qualitatively the same, although quantitatively less pronounced. However, there is still some uncertainty as to whether fixed oxide traps act to decrease or increase μ in p-channel devices. The former is argued by Zupac et al. [20] and has been observed by others as well [21,22]. The latter has been demonstrated by S. Dimitrijev and N. Stojadinovic et al. [23] and attributed to decreased surface-roughness scattering in the presence of fixed oxide traps. In order to confirm one of these models, one has to study p-channel devices in which interface trap creation is negligible in comparison with fixed oxide trap creation. Unfortunately, as the $\Delta N_{ft}/\Delta N_{st}$ ratio is found to be (unexpectedly) high in both types of RADFETs studied here, the predominant effect of ΔN_{st} obscures the effect of ΔN_{ft}. In addition, the contribution of switching oxide traps to ΔN_{st} complicates even quantification of the effects of interface traps on μ. Consequently, no conclusion about ΔN_{ft} effects on μ can be made based on the obtained data. Indeed, it can be seen in Figs. 9 and 10 that μ generally follows the pattern of inverse ΔN_{st} (ΔN_{st} is shown in Figs. 11b-14b).

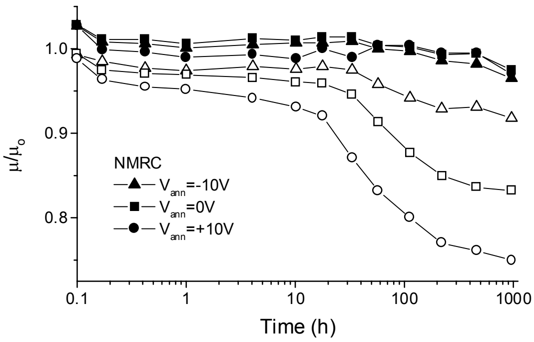

Fig. 9. NMRC samples: μ/μ_o during annealing at 100°C with negative, zero and positive gate bias; solid symbols - zero irradiation bias, open symbols - positive irradiation bias (+5V).

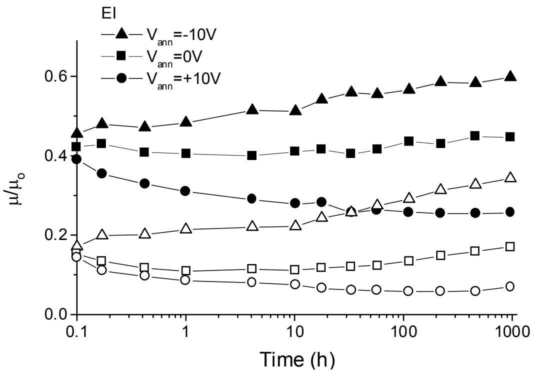

Fig. 10. EI samples: μ/μ_o during annealing at 100°C with negative, zero and positive gate bias; solid symbols - zero irradiation bias, open symbols - positive irradiation bias (+5V).

Figs. 11 and 12 show ΔN_{ft} and ΔN_{st} during annealing for NMRC samples for the case of zero and positive V_{irr}, respectively. The positive V_{ann} enhances formation of switching traps and decay of fixed traps. The ΔN_{ft} even goes into the negative region, particularly in V_{irr}=0V case. Note that there is still a qualitative agreement between ΔN_{st} values obtained by CPT and MGT. Moreover, the changes in ΔN_{st} during annealing as determined by the two techniques are roughly the same.

Finally, Figs. 13 and 14 show the same data as Figs. 11 and 12, but for EI samples. The ΔN_{ft} pattern is qualitatively similar to that in NMRC samples (positive V_{ann} enhances the decrease of ΔN_{ft}). However, there are some quantitative differences, such as larger magnitude of negative ΔN_{ft} observed for both V_{irr}=0 and +5V, particularly in the case of V_{ann}=+10V. As to ΔN_{st}, opposite to the pattern observed in NMRC samples, there is even an absence of ΔN_{st}(MGT) and ΔN_{st}(CPT) qualitative agreement, again particularly for V_{ann}=+10V. Generally, ΔN_{st}(CPT) stays little changed, while ΔN_{st}(MGT) increases substantially (V_{ann}=+10V) or decreases (e.g. V_{irr}=+0V, V_{ann}=-10V in Fig. 13b).

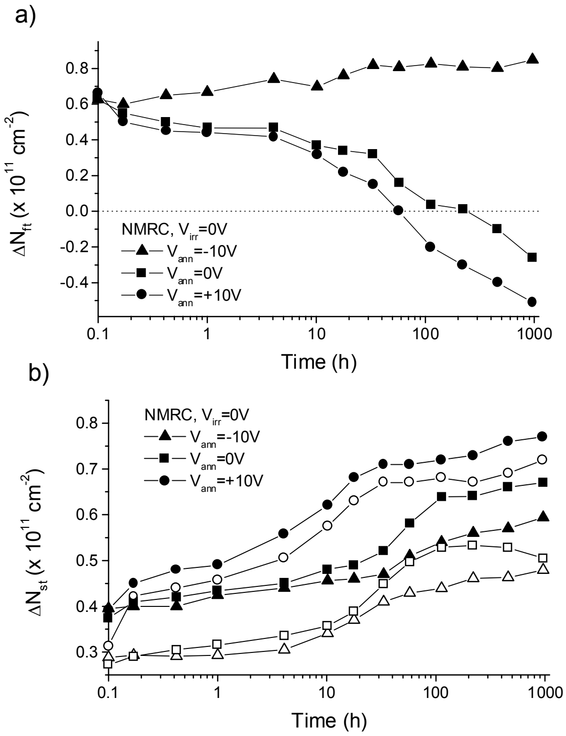

Fig. 11. NMRC samples: ΔN_{ft} (a) and ΔN_{st} (b; MG-solid symbols, CP-open symbols) during annealing at 100°C with negative, zero and positive gate bias; zero irradiation bias.

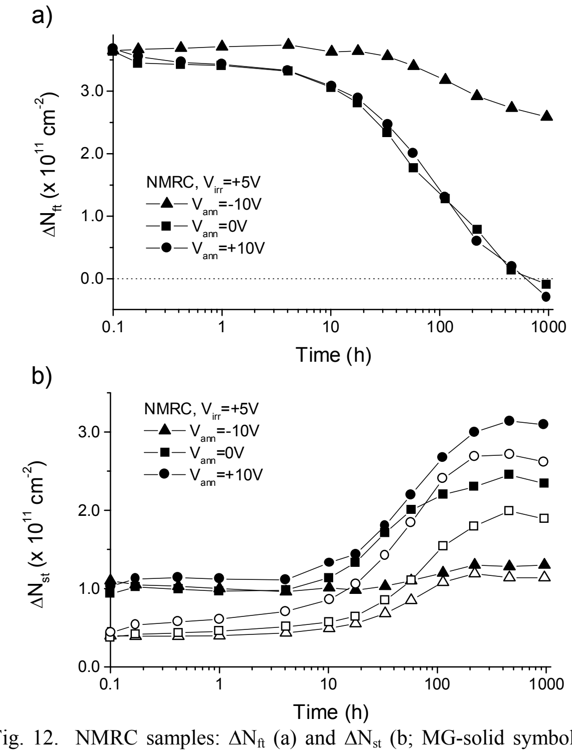

Fig. 12. NMRC samples: ΔN_{ft} (a) and ΔN_{st} (b; MG-solid symbols, CP-open symbols) during annealing at 100°C with negative, zero and positive gate bias; positive irradiation bias (+5V).

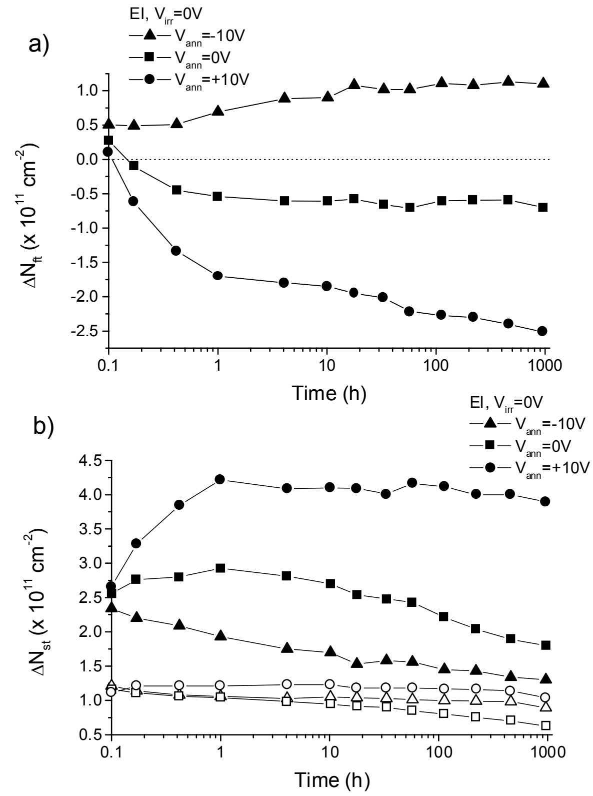

Fig. 13. EI samples: ΔN_{ft} (a) and ΔN_{st} (b; MG-solid symbols, CP-open symbols) during annealing at 100°C with negative, zero and positive gate bias; zero irradiation bias.

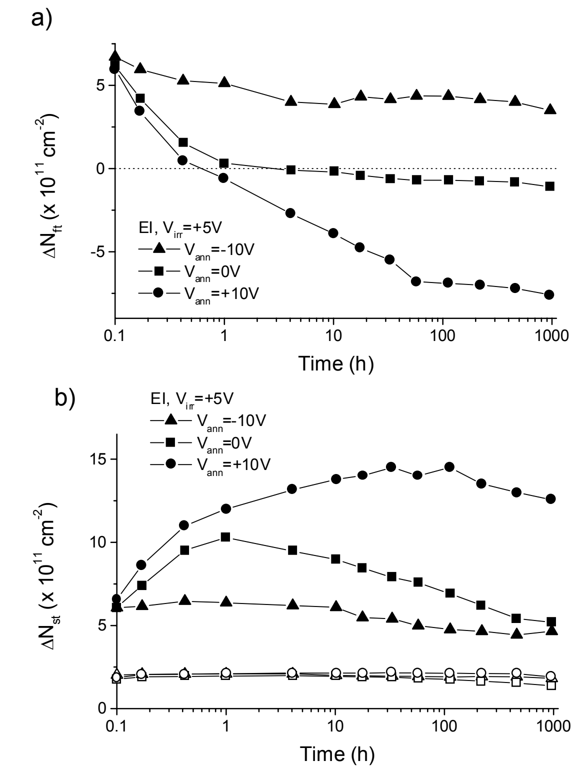

Fig. 14. EI samples: ΔN_{ft} (a) and ΔN_{st} (b; MG-solid symbols, CP-open symbols) during annealing at 100°C with negative, zero and positive gate bias; positive irradiation bias (+5V).

C. Microscopic Mechanisms

Presented experimental results can be most readily explained within the general context of the HDL model [24,25,26]. The crucial role in this model belongs to the E_γ' centre, which is a weak Si-Si bond in the oxide caused by an oxygen atom vacancy between two Si atoms, each back-bonded to three oxygen atoms [27]. The E_γ' centre acts as a hole trap and is predominantly responsible for the increase of oxide trapped charge during irradiation [28]. As discussed in Section II, the oxide trapped charge involves both charge trapped at fixed oxide traps and that trapped at switching oxide traps. Namely, under the influence of the positive electric field in the oxide (caused by positive gate bias) during annealing, the hole trapped at the E_γ' centre can be either compensated or neutralised by the electron tunnelling from Si. In the case of compensation, when the negative field (negative gate bias) is applied, the electron can tunnel back to Si, leaving the E_γ' centre positively charged. Thus, some of the E_γ' centres can communicate electrically with Si, the communication being easier and faster in case they are closer to the Si/SiO_2 interface. We will accept convincing arguments of Lelis and Oldham [26] that the switching oxide traps in irradiated oxides are E_γ' centres close to the Si/SiO_2 interface. The fixed oxide traps are microscopically E_γ' centres as well, however further from the Si/SiO_2 interface and hence incapable of exchanging charge with Si during the time frame of the measurements.

The negative ΔN_{ft} observed at certain bias conditions in both NMRC and EI samples indicates that there is also negative charge, i.e. electron trapping in the oxide. Such phenomenon has been observed previously in MOSFET oxides and its importance in radiation response demonstrated [29-32]. Electron trapping can also be attributed to E_γ' centres [26]. Namely, it has been proposed [33,26] that, under appropriate conditions, the compensated E_γ' centre can capture a second electron and become net negative. In other words, after electron capture, E_γ' centre becomes an amphoteric trap that can either release or capture an electron and become positively or negatively charged, respectively.

As discussed in Section II, the MGT is a slow technique that registers both interface traps and near-interfacial switching oxide traps (E_γ' centres) as switching traps. The much faster CPT registers as switching traps the interface traps and perhaps only the fastest switching oxide traps, i.e. the E_γ' centres closest to the Si/SiO_2 interface that can not be distinguished from interface traps. Thus, the CPT can be used for at least rough estimation of the interface trap behaviour, and. combination of MGT and CPT in some cases may provide information about switching oxide traps.

It is clear that ΔN_{ft}, ΔN_{sot} and ΔN_{it} all increase during irradiation. The exact proportion between ΔN_{sot} and ΔN_{it} during irradiation is difficult to determine, but it is probable that a significant part of ΔN_{st} in NMRC samples and dominant part of ΔN_{st} in EI samples is due to switching oxide traps. This would be in line with observations of Fleetwood et al. [17] in soft oxides.

The ΔN_{ft} behaviour during annealing (Figs. 11a-14a) is consistent with DHL model. For example, for V_{ann}=-10V, ΔN_{ft} increases (V_{irr}=0V) or decreases slightly (V_{irr}=+5V) in both NMRC and EI samples. The increase for V_{irr}=0V is due to tunnelling of trapped holes from E_γ' centres to Si under the influence of negative electric field at the Si/SiO_2 interface. The slight decrease for V_{irr}=+5V indicates that the built-in positive field in the vicinity of the interface due to radiation-induced positive charge is stronger than the negative filed caused by V_{ann}, enabling the electrons to tunnel from Si to E_γ' centres and neutralise the holes trapped there. As expected, much more pronounced ΔN_{ft} decrease is observed for V_{ann}=0 and +10V, which both correspond to the positive electric field at the Si/SiO_2 interface, the field being greater in magnitude in the latter case and hence ΔN_{ft} decrease being enhanced. Besides neutralisation of charge trapped at E_γ' centres by electrons tunnelling from Si under the influence of electric field, the electrons thermally emitted from the oxide valence band also contribute to E_γ' centres neutralisation [34]. Finally, electron trapping is another mechanism causing ΔN_{ft} decrease. Electron trapping is more pronounced in EI samples, and, as expected, for positive V_{ann}.

If we consider ΔN_{st} behaviour during annealing (Figs. 11b-14b), in NMRC samples there is ΔN_{st}(MGT) increase closely followed by ΔN_{st}(CPT) increase. The parallel offset between ΔN_{st}(MGT) and ΔN_{st}(CPT) implies that there is a genuine increase in interface traps during annealing and that the number of switching oxide traps stays roughly unchanged. This is consistent with previous results by Fleetwood et al. [17]. The build-up of interface traps during irradiation and annealing can be explained by the so called hydrogen models [16], which involve release of hydrogenous species (H^+ ions [35] and/or H_2 molecules [36]) in the oxide, their transport to the Si/SiO_2 interface and reactions in which interface traps are formed. According to hydrogen models, details of interface traps behaviour are determined by the hydrogen content of the oxide and V_{ann} (both increased hydrogen content and positive V_{ann} enhance formation of interface traps). Interface trap models will not be elaborated in detail here, the reader is referred to the original work [35,36].

In EI samples, ΔN_{st}(CPT) is roughly constant during annealing, implying that there is little or no change in ΔN_{it}, and, hence, ΔN_{st}(MGT) behaviour approximates that of ΔN_{sot}. For V_{ann}=+10V, similar to NMRC samples, there is a substantial increase in ΔN_{st}(MGT). However, in contrast to NMRC samples, ΔN_{st}(MGT) increase is due to switching oxide traps, and not interface traps. The patterns of ΔN_{ft}, ΔN_{sot} and ΔN_{it} behaviours during annealing with V_{ann}=+10V are summarised in Table 2.

TABLE II

NMRC AND EI SAMPLES: ΔN_{FT}, ΔN_{SOT} AND ΔN_{IT} PATTERNS DURING ANNEALING WITH V_{ANN}=+10V.

	ΔN_{ft}	ΔN_{it}	ΔN_{sot}
NMRC	↓	↑	↔
EI	↓	↔	↑

For V_{ann}=-10V, there is a decrease in ΔN_{st}(MGT). The decrease is more pronounced in the case of V_{irr}=0V than V_{irr}=+5V, most probably because the resultant field at the Si/SiO_2 interface is more negative in the former case owing to less positive charge trapped (compare ΔN_{ft} in Figs. 13a and 14a). For an intermediate case of V_{ann}=0V, initial increase in ΔN_{st}(MGT) is followed by a decrease at later annealing times. The turn-around point is at the time when the electric field at the Si/SiO_2 interface, primarily determined by the sign of ΔN_{ft}, turns negative (see e.g. Fig. 14b). It seems that in EI samples the electric field at the interface determines switching oxide traps behaviour: positive field acts to increase ΔN_{sot}, while negative field acts to decrease ΔN_{sot}. This can be explained by assuming that tunnelling of electrons from Si to the E_γ' centres under the positive bias results in creation of switching oxide traps. Oppositely, tunnelling of electrons from E_γ' centres to Si leaves the centres in the state in which they cannot exchange charge with Si during the measurements. Microscopically, all these defects are related to the E_γ' centres, but the capture or release of electron changes the energy level and thereby the nature of the centre. Physical location of the centres and their energy levels may differ from oxide to oxide, causing different radiation responses as observed in our study.

D. *Effects of processing steps*

Differences in details of the radiation response of NMRC and EI samples (see e.g. Table 2) are the consequence of different parameters of processing steps used during fabrication of experimental samples. It is not easy to unambiguously determine which particular process step is crucial for the explanation of the radiation response, as the response is often determined not only by the individual step, but by the process sequence within which it occurs [16]. Nevertheless, general impact of certain steps has been documented and can be analysed.

As E_γ' centres are argued to have a dominant role in hole and electron trapping at both fixed or switching traps in the oxides investigated here, we will discuss the process steps crucial for E_γ' centres formation. It has been shown [37] that the formation of E_γ' centres is predominantly affected by the highest temperature used in the process flow. In our case of Al-gate devices it is the oxidation temperature. In addition, the post-oxidation anneal (POA) step has been shown to be of the most importance for the switching oxide trap behaviour. Both oxidation and POA were performed at higher temperatures in EI samples, and the POA duration was longer as well. Increased oxidation temperature, POA temperature and POA duration all act to increase the number of E_γ' centres in the oxide [38,39]. This may be the explanation for higher radiation sensitivity due to increased charge trapping in EI samples, as well as for generally more pronounced changes in ΔN_{ft} and ΔN_{st} during annealing. On the other hand, it has been argued [37-39] that the higher temperature POA relieves the strain in the vicinity of the Si/SiO_2 interface. Within the context of DHL model, relieved strain leads to the smaller number of E_γ' centres that act as switching oxide traps, while it doesn't necessarily mean smaller total number of E_γ' centres [26,40]. Such oxides would exhibit slower decay of ΔN_{ft} during annealing [40], which is not observed in our case. Perhaps the reason for this discrepancy is in the complex influence of not only individual process steps but also certain process sequences on location and energy levels of the traps in the oxide. The problem is also in the inability of the employed characterisation techniques to provide information about some pertinent details of the microscopic processes that occur during irradiation and annealing. For example, it still cannot be distinguished by CPT with complete certainty whether the ΔN_{it} increase in NMRC samples (Figs. 11b and 12b) is really entirely due to interface traps or to switching oxide traps very near the Si/SiO_2 interface. Similarly, the effects of hole and electron trapping are both contained in ΔN_{ft} data and cannot be separated using MGT. In addition, the MGT can be sensitive to lateral non-uniformities (LNUs) in the trapped charge distribution in the oxide [41], which may further complicate precise quantification of the ΔN_{st} contribution.

IV. CONCLUSIONS

Radiation and post-irradiation responses of the two types of low sensitivity/high dose range RADFETs have been investigated. Measurements in practical applications and during RADFET calibration typically involve determination of the threshold voltage only in a single specified point of the device I-V characteristic. While such procedure is confirmed to be sufficient from the application point of view, RADFET further development requires insight into microscopic processes that occur during irradiation and subsequent annealing. This study has demonstrated the use of sub-threshold midgap and charge pumping techniques in RADFETs. Admittedly, these electrical techniques have limitations, such as that they cannot provide information of the microscopic structure of the defects in the oxide and at the Si/SiO_2 interface, cannot clearly distinguish the contributions of electrons and holes to the charge trapped in the oxide, or are sensitive to LNUs (MGT). However, concurrent use of MGT and CPT can still provide valuable information about the effects of switching oxide traps and interface traps, which are indistinguishable when a single technique (e.g. MGT is used). The knowledge about behaviour patterns of interface traps, switching oxide traps, together with that of fixed oxide traps, is crucial in optimising the RADFET response. Often complex interplay between these three types of traps determines radiation sensitivity and post-irradiation stability (fading). That explains, for instance, somewhat unexpected result in Figs. 7 and 8 that fading is lower for V_{ann}=+10V than for V_{ann}=0V. (It is expected that the fading for V_{ann}=-10V is the lowest.) Switching oxide traps are particularly important in RADFETs as they have the dominant influence on another important parameter – a short-term drift [42].

It has been proposed that the E_γ' centres play the crucial role in RADFET response, being responsible for both fixed and switching traps in the oxide and for both hole and electron trapping. Therefore, the need to optimise the RADFET fabrication process in terms of E_γ' centres number, location and energy is of paramount importance. This can be done by optimisation of the highest temperature processes, i.e. usually gate oxidation and subsequent anneal in an inert atmosphere. However, one should be careful when making conclusions because sometimes the whole process sequence rather than individual process steps can have an impact on radiation and post-irradiation response of the devices.

Another approach to optimising the RADFET response would be the use of oxide-nitride structures instead of standard, thermal gate oxides [43,44]. These RADFETs operate with negative bias applied on the gate, and the charge trapping does not occur at the Si/SiO_2 interface, but at the SiO_2/Si_3N_4 interface. The role of electron tunnelling, and, consequently, Eγ' centres, is not crucial in these devices, and they should exhibit superior fading and drift characteristics [43,44]. However, as the charge is trapped further from the Si/SiO_2 interface, such RADFETs would in general be less sensitive, limiting their use to high dose applications with stringent fading requirements.

V. References

[1] A. Holmes-Siedle, "The space-charge dosimeter," *Nucl. Instrum. Methods*, vol. 121, pp. 169-179, 1974.

[2] A. Holmes-Siedle and L. Adams, "RADFET: a review of the use of metal-oxide-silicon devices as integrating dosimeters," *Radiat. Phys. Chem.*, vol. 28, pp. 235-244, 1986.

[3] A. Kelleher, N. McDonnell, B. O'Neill, L.Adams, and W. Lane, "The effect of gate oxide process variations on the long-term fading of the PMOS dosimeters," *Sensors and Actuators A*, vol. 37-38, pp. 370-374, 1993.

[4] D.J. Gladstone, X.Q. Lu, J.L. Humm, H.F. Bowman, and L.M. Chin, "Miniature MOSFET radiation dosimeter probe," *Med. Phys.*, vol. 21, pp. 1721-1728, 1994.

[5] G.F. Knoll, *Radiation detection and measurement*, Wiley, New York, 1989.

[6] G. Polge, L. Dusseau, K. Idri, D. Plattard, J. Fesquet, J. Gasiot, and N. Iborra-Brassar, "Characterisation of a 63 MeV proton beam with optically stimulated luminescent films," *Proc. RADECS 2001 Conference*, paper A-1, in press.

[7] D. Plattard, L. Dusseau, J.R. Vaille, G. Ranchoux, G. Polge, J. Fesquet, R. Ecoffet, and J. Gasiot, "Characterisation of an integrated sensor using optically stimulated luminescence for in flight dosimetry," *Proc. RADECS 2001 Conference*, paper A-2, in press.

[8] B. O'Connell, C. Conneely, C. McCarthy, J. Doyle, W. Lane, and L. Adams, "Electrical performance and radiation sensitivity of stacked PMOS dosimeters under bulkbias control," *IEEE Trans. Nucl. Sci.*, vol. 45, pp. 2689-2694, 1998, and references therein.

[9] www.nmrc.ie/projects/radfets/index.html

[10] S.M. Sze, *Physics of Semiconductor Devices*, Wiley, New York, 1981.

[11] G. Ristic, M. Pejovic, and A. Jaksic, "PMOS dosimetric transistors with two-layer gate oxide," *Sensors and Actuators A*, vol. 63, pp. 129-134, 1997, and references therein.

[12] P.J. McWhorter and P.S. Winokur, "Simple technique for separating the effects of interface traps and trapped-oxide charge in metal-oxide-semiconductor transistors," *Appl. Phys. Lett.*, vol. 48, pp. 133-135, 1986.

[13] G. Groeseneken , H.E. Maes, N. Beltran, and R.F. De Keersmaecker, "A reliable approach to charge-pumping measurements in MOS transistors," *IEEE Trans. Electron Dev.*, vol. 31, pp. 42-53, 1984.

[14] B.M. Elliot, "The use of charge pumping currents to measure surface state densities in MOS transistors," *Solid-State Electron.*, vol 19, pp. 241-247, 1976.

[15] D.M. Fleetwood, "Border traps in MOS devices," *IEEE Trans. Nucl. Sci.*, vol. 39, pp. 269-271, 1992.

[16] T.P. Ma and P.V. Dressendorfer, *Ionizing radiation effects in MOS devices and circuits*, Wiley, New York, 1989.

[17] D.M. Fleetwood, M.J. Johnson, T.L. Meisenheimer, P.S. Winokur, W.L. Warren, and S.C. Witczak, "1/f noise, hydrogen transport and latent interface-trap buildup in irradiated MOS devices," *IEEE Trans. Nucl. Sci.*, vol. 44, pp. 1810-1817, 1997.

[18] K.F. Galloway, M. Gaitan, and T.J. Russell, "A simple model for separating interface and oxide charge effects in MOS device characteristics," *IEEE Trans. Nucl. Sci.*, vol. 31, pp. 1497-1501, 1984.

[19] D.M. Fleetwood, M.R. Shaneyfelt, J.R. Schwank, P.S. Winokur, and F.W. Sexton, "Theory and application of dual-transistor charge separation analysis," *IEEE Trans. Nucl. Sci.*, vol. 36, pp. 1816-1824, 1989.

[20] D. Zupac, K.F. Galloway, P. Khosropour, S.R. Anderson, and R.D. Schrimpf, "Separation of effects of oxide-trapped charge and interface-trapped charge on mobility in irradiated power VDMOSFETs," *IEEE Trans. Nucl. Sci.*, vol. 40, pp. 1307-1315, 1993, and references therein.

[21] F.B. McLean and H.E. Boesch, Jr., "Time-dependent degradation of MOSFET channel mobility following pulsed irradiation," *IEEE Trans. Nucl. Sci.*, vol. 36, pp. 1772-1783, 1989.

[22] N.S. Saks, R.B. Klein, and D.L. Griscom, "Formation of interface traps in MOSFETs during annealing following low temperature irradiation," *IEEE Trans. Nucl. Sci.*, vol. 35, pp. 1234-1240, 1988.

[23] S. Dimitrijev and N. Stojadinovic, "Analysis of CMOS transistor instabilities," *Solid-State Electron.*, vol. 30, pp. 991-1003, 1987.

[24] A.J. Lelis, H.E. Boesch, Jr., T.R. Oldham, and F.B. McLean, "Reversibility of trapped hole annealing," *IEEE Trans. Nucl. Sci.*, vol. 35, pp. 1186-1191, 1988.

[25] A.J. Lelis, T.R. Oldham, H.E. Boesch, Jr., and F.B. McLean, "The nature of the trapped hole annealing process," *IEEE Trans. Nucl. Sci.*, vol. 36, pp. 1808-1815, 1989.

[26] A.J. Lelis and T.R. Oldham, "Time dependence of switching oxide traps," *IEEE Trans. Nucl. Sci.*, vol. 41, pp. 1835-1843, 1994.

[27] F.J. Feigl, W.B. Fowler, and K.L. Yip, "Oxygen vacancy model for the E'_1 center in SiO_2," *Solid-State Commun.*, vol. 14, pp. 225-229, 1974.

[28] P.M. Lenahan and P.V. Dressendorfer, "Hole traps and trivalent silicon centers in metal/oxide/silicon devices," *J. Appl. Phys.*, vol. 55, pp. 3495-3499, 1984.

[29] D.M. Fleetwood, P.S. Winokur, R.A. Reber, Jr., T.L. Meisenheimer, J.R. Schwank, M.R. Shaneyfelt, and L.C. Riewe, "Effects of oxide traps, interface traps and border traps on metal-oxide-semiconductor devices," *J. Appl. Phys.*, vol. 73, pp. 5058-5074, 1993.

[30] V.S. Pershenkov, V.V. Belyakov, S.V. Cherepko, A.Y. Nikiforov, A.V. Sagoyan, V.N. Ulimov, and V.V. Emelianov, "Effect of electron traps on reversibility of annealing," *IEEE Trans. Nucl. Sci.*, vol. 42, pp. 1750-1757, 1995.

[31] V.S. Pershenkov, S.V. Cherepko, A.V. Sagoyan, V.V. Belyakov, V.N. Ulimov, V.V. Abramov, A.V. Shalnov and V.I. Rusanovsky, "Proposed two-level acceptor-donor (AD) center and the nature of switching traps in irradiated MOS structures," *IEEE Trans. Nucl. Sci.*, vol. 43, pp. 2579-2586, 1996.

[32] D.M. Fleetwood, P.S. Winokur, L.C. Riewe, O. Flament, P. Paillet, and J.L. Leray, "The role of electron transport and trapping in MOS total-dose modeling," *IEEE Trans. Nucl. Sci.*, vol. 46, pp. 1519-1525, 1999.

[33] M. Walters and A. Reisman, "Radiation-induced neutral electron trap generation in electrically biased insulated gate filed effect transistor gate insulators," *J. Electrohem. Soc.*, vol. 138, pp. 2756-2762, 1991.

[34] P.J. McWhorter, S.L. Miller, and W.M. Miller, "Modeling the anneal of radiation-induced trapped holes in a varying thermal environment," *IEEE Trans. Nucl. Sci.*, vol. 37, pp. 1682-1689, 1990.

[35] D.B. Brown and N.S. Saks, "Time dependence of radiation-induced interface trap formation in metal-oxide-semiconductor devices as a function of oxide thickness and applied field," *J. Appl. Phys.*, vol. 70, pp. 3734-3747, 1991, and references therein.

[36] R.E. Stahlbush, A.H. Edwards, D.L. Griscom, and B.J. Mrstik, "Post-irradiation cracking of H_2 and formation of interface states in irradiated metal-oxide-semiconductor field-effect transistors," *J. Appl. Phys.*, vol. 73, pp. 658-667, 1993, and references therein.

[37] P.M. Lenahan, J.J. Mele, J.F. Conley, Jr., R.K. Lowry, D. Woodbury, "Predicting radfiation response from process parameters: verification of a physically based predictive model," *IEEE Trans. Nucl. Sci*., vol. 46, pp. 1534-1543, 1999.
[38] J.R. Schwank and D.M. Fleetwood, "Effect of post-oxidation anneal temperature on radiation-induced charge trapping in metal-oxide-semiconductor devices," *Appl. Phys. Lett*., vol. 53, pp. 770-772, 1988.
[39] W.L. Warren, D.M. Fleetwood, M.R. Shaneyflet, J.R. Schwank, P.S. Winokur, R.A.B. Devine and D. Mathiot, "Links between oxide, interface, and border traps in high-temperature annealed Si/SiO_2 systems," *Appl. Phys. Lett*., vol. 64, pp. 3452-3454, 1994.
[40] T.R. Oldham, A.J. Lelis, and F.B. McLean, "Spatial dependence of trapped holes determined from tunneling analysis and measured annealing," *IEEE Trans. Nucl. Sci*., vol. 33, pp. 1203-1209, 1986.
[41] R.K. Freitag, E.A. Burke, C.M. Dozier, and D.B. Brown, "The development of non-uniform deposition of holes in gate oxides," *IEEE Trans. Nucl. Sci*., vol. 35, pp. 1203-1207, 1988.
[42] Z. Savic, B. Radjenovic, M. Pejovic, and N. Stojadinovic, "The contribution of border traps to threshold voltage shift in pMOS dosimetric transistors," *IEEE Trans. Nucl. Sci*., vol. 42, pp. 1445-1454, 1995.
[43] R.C. Hughes, W.R. Dawes, Jr., W.J. Meyer, and S.W. Yoon, "Dual dielectric silicon metal-oxide-semiconductor field-effect transistors as radiation sensors," *J. Appl. Phys.*, vol. 65, pp. 1972-1976, 1989.
[44] J.R. Schwank, S.B. Boeske, D.E. Beutler, D.J. Moreno, and M.R. Shaneyfelt, "A dose rate independent PMOS dosimeter for space applications," *IEEE Trans. Nucl. Sci*., vol. 43, pp. 2671-2678, 1996.